Egypt. J. Chem. **Vol. 66,** No. 6 pp. 331 - 342 (2023)

+

Egyptian Journal of Chemistry

http://ejchem.journals.ekb.eg/

Hydrogeochemical studies of the groundwater at the flood plain Quaternary aquifer in Beni suef area, Egypt

Mahmoud Awad [1]*, Essam A. Mohamed [1], Shaban G. Saber [2], Mohamed Mokhtar Yehia [3], El Sayed El Bastamy El Sayed [3], Tamer Nassar [4]

[1] *Hydrogeology and Environment Department, Faculty of Earth Sciences, Beni-Suef University, Beni-Suef, Egypt.*

[2] *Geology Department, Faculty of Science, Beni-Suef University, Beni-Suef, Egypt.*

[3] *Central Laboratory for Environmental Quality Monitoring, National Water Research Center, Kanater El-Khairia, Egypt*

.[4] *Geology Department, Faculty of Science, Cairo University, Cairo, Egypt*.

Abstract

Quaternary deposits represent the main aquifer in the investigated region. Currently Groundwater contamination has become an important issue. The goal of this research is to determine the hydrochemical properties and the impact of anthropogenic activity on the groundwater. To do that, 40 water samples from surface and groundwater were collected and examined for major ions and trace elements. The western regions of the area have high TDS, Na, Ca, SO4, and Cl levels, indicating the presence of local pollution sources arising from the seepage from household, agricultural, and industrial wastes of a densely populated area. The concentration of iron, cadmium, aluminum, and manganese are above permissible levels at most of the groundwater area. Piper and Chadha diagrams revealed that The water type evolved from Ca–Mg–HCO3 in Nile waters to Na–Cl–SO4 at the western side, and then from Na–Cl–SO4 to Ca–Mg–HCO3 due to the dilution and mixing of (Ca–Mg–HCO3) infiltrated water from (EL-Ibrahimia canal, irrigation canals and agriculture land). The PCA, binary plots, and saturation indices revealed that weathering of carbonates and evaporites, cation exchange, and human activities are the main factors behind the geochemical evolution of groundwater.

Keywords: Groundwater chemistry modeling; Principal component analysis; Quaternary Aquifer; Water rock interaction; Groundwater contamination.

1. Introduction:

The Floodplain groundwater aquifer is important for providing water demands for residential, agricultural, and industrial uses in Egypt. Nile floodplain aquifers are semi-confined that are particularly vulnerable to pollution and contamination since they are located in urban and heavily cultivated rural regions[1]. To recognize groundwater quality and expect the pollution source, it is important to study the geochemical evolution of the groundwater along its way from the recharge to discharge sites.

In recent years, determination of the quality and accessibility of fresh groundwater for various uses is becoming increasingly important. The current study will focus on the floodplain aquifer to find the extent of the effect of various activities on the groundwater quality in addition to the water-rock interaction process. Nile water feeds this aquifer to a large extent. So, studying the hydrochemical characteristics of groundwater, the geochemical processes involved, and its evolution under natural water circulation processes is critical not only for determining the most efficient use and protection of this valuable resource, but also for predicting changes in the groundwater environment [2, 3].

The study area is located in Beni-Suef Governorate, covers an area of about 10951 km^2 and is bordered by the Western and Eastern Deserts (Fig. 2). Around 12% of the area is inhabited, while the remaining percentage 88% is desert lands. Agricultural fields account for about 85 % of the entire population. The governorate of Beni Suef is located between the latitudes of 28° 45° N and 29° 25° N, and the longitudes of 30° 45° E and 31° 15° E. in addition to the artificial irrigation canals, which cover a large part like Al Ibrahimia, Baher Youssef (Fig. 2), but the groundwater from the Quaternary flood plain aquifer represents an significant source of domestic and farming uses in many areas of this region.

According to [4], the groundwater at the South western part has a high salinity with significant concentration of nutrients and heavy metals including

*Corresponding author e-mail: mahmoudawad1444@gmail.com. (Mahmoud Awad)

Receive Date: 12 April 2022, Revise Date: 19 September 2022, Accept Date: 20 September 2022

DOI: 10.21608/EJCHEM.2022.132791.5877

Mn, Fe, Cd, and Ba, which exceed the acceptable limits of drinking water. [5] recognized a pollution by Cd, Al , Mn, Fe, Cu, and Co in the groundwater. Fertilizers and pesticides, trash disposal and industrial wastes, leakage from septic tanks, wastewater leaked from El-Moheet drain, and evaporation processes were all mentioned as possible contamination causes related to anthropogenic activity.

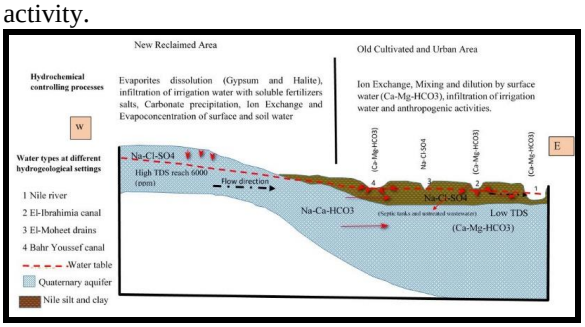

Figure 1. Schematic abstract showing the hydrogeochemical evolution of ground water and there controlling processes in the investigated area.

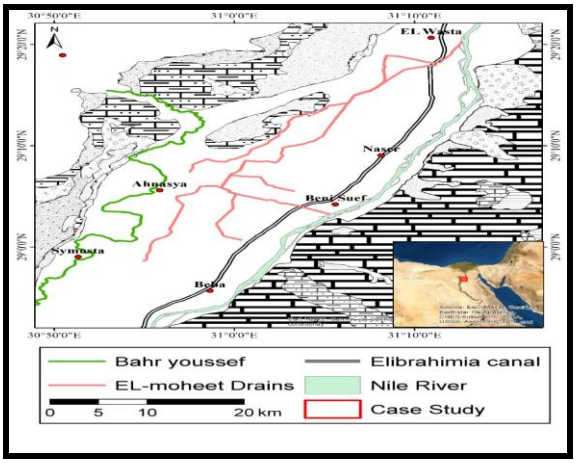

Figure 2. Location map of the study area.

Geologic setting:

Almost all the exposed rocks and sediments in Beni Suef Governorate are of sedimentary origin. The surface and sub-surface geologic characteristics of the Nile valley have a vital importance for detecting the hydrogeologic pattern in term of aquifer characteristics, water potentiality, and flow. Brief description of the lithostratigraphic sequence will be considered in the following section (Figs.3 and 4).

. Surface stratigraphic sequence:

The exposed rock units in the investigated area from the more recent to those sediment in earlier periods (Fig. 3) are; Holocene silt and clay forming the cultivated Nile flood plain, Pleistocene sand and gravels forming elongated strip extended between the flood plain and the valley slopes, and the Eocene limestone which are encountered in subsurface and exposed at Eastern and western side of the flood plain forming rocky plateau [6].

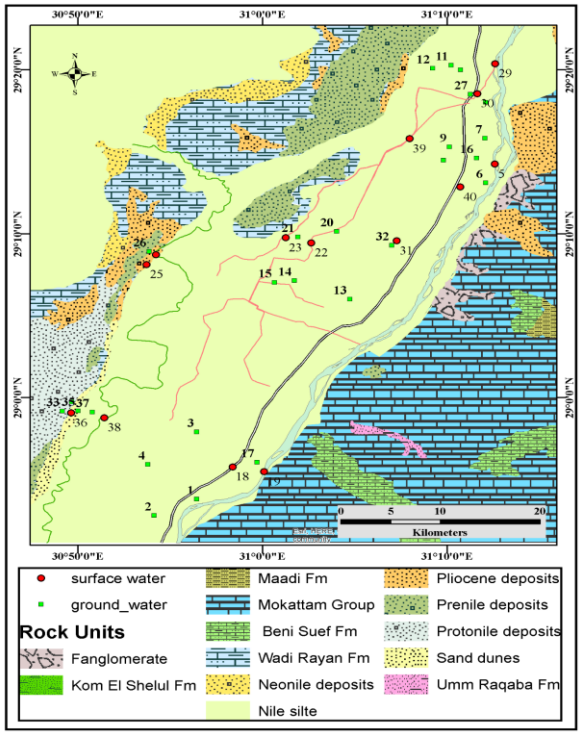

Figure 3. Geological map of Beni Suef region Modified after [6].

Subsurface stratigraphic sequence:

The subsurface stratigraphic sequence was compiled by [7]through several drilled wells in Beni Suef area (Fig.4). The lithological description of the rock units is discussed as following from old to young:

- **Middle Eocene Deposits:** They are formed of fractured limestone and grey marls with thin shale and clay intercalations.
- **Pliocene deposits**: They recognized as a thick impermeable to semi permeable zone overlie the Middle Eocene rocks and underlie the Quaternary sediments. They are composed of clays and shales.
- **Plio-Pleistocene Deposits:** They overlie on the Pliocene clays and shales and made up of interbedded layers of sand and clays with gravels.
- **Pleistocene deposits**: it contained graded sands and gravels with clay lenses. They are directly underlying the Holocene Nile silts and sands. They represent the Quaternary aquifer.

Holocene deposits: These deposits represent the top most rock unit in the Nile Valley and Delta. They are composed of silts and fine sands. They form the overlying semi permeable layers for the Quaternary aquifer.

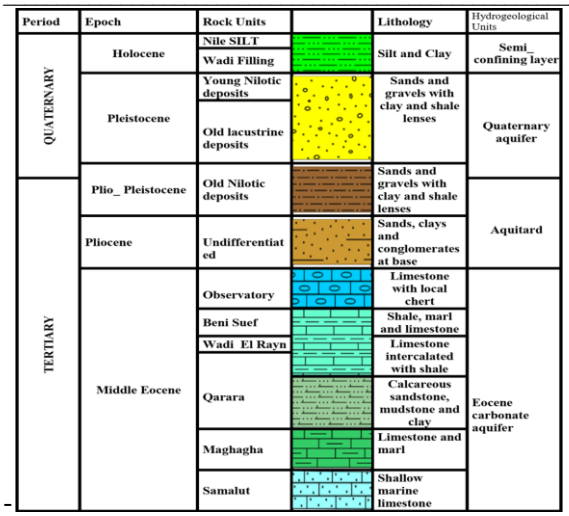

Figure 4. Subsurface lithostratigraphic rock units, with hydrogeological definition [8].

Hydrogeological setting:

Surface water System

The surface water hydrology in the Beni Suef region is represented by the main course of the Nile River, the drains, and the irrigation canals. El Ibrahimia and Bahr Yousef canals, which receive their water straight from the Nile River, are the principal irrigation canals. The two canals were built along the Nile Valley's western flood plain. The unique drain is Elmoheet drain (Fig. 3).

Water balance model of Beni Suef governorate

the available water resources from surface water (Baher Youssef and El Ibrahimia Canal) about ~ 2.146 B m^3/y and groundwater ~ 0.02 Bm^3/y (Table.1), along with all outputs from the water system to the different sectors, and the amount of water drained into the Nile River and the water lost by evaporation. The balance also shows the water needs of all sectors, what is actually consumed and what is returned to the system. Where the total household needs in Beni Suef in 2016 amounted to ~ 0.177 B m^3/y while the industrial sector need about ~ 0.017 B m^3/y, in addition to ~ 0.006 B m^3/y taken directly from the Nile water returned to the system as treated sewage ~ 0.054 B m^3/y, amount of the returned water ~ 0.011 B m^3/y are used for planting tree forests and untreated sewage ~ 0.111 B m^3/y. The agricultural needs of surface water reach ~ 2,009 Bm^3/y for irrigation 363,480 hectare are actually consumed ~ 1.205Bm^3/y and the rest is up to the system. In addition to the needs of agriculture for supplementary irrigation, about 0.06 B m^3/y, which is about 0.051 Bm^3/y of surface water and ~ 0.009 Bm^3/y of groundwater to irrigate the reins of 10996 acres. Agriculture from the only groundwater irrigation ~ 0.014 B m^3 annually to irrigate~ 2524 hectare, and actually consumes ~ 0.013 Bm^3/y annually. The amount of losses by infiltration from the canal network was estimated at about 0.1 Bm^3/y annually. One of the most important outputs of the water balance is the amount of agricultural wastewater reused to fill the water deficit, which is estimated at about 0.077 Bm^3/y.

Table 1 **.** Water balance model of Beni Suef governorate.

Water resources	volume (Bm3/year)	sector	The Consumption volume (Bm3/year)	The used volume (Bm3/year)
Traditional water resources		household needs	.012	0.177
El Ibrahimia Canal and Baher Youssef	2.146	Industry	.002	0.023
		agricultural needs	1.205	2.009
		Agriculture based on groundwater	0.049	0.047
The Nile River directly (drinking water)	0.117	Drained water to the desert and forests	.012	
		Evaporation	0.1	
Deep ground water	.023	Drained water to the Nile river	0.906	
Total volume (Bm3/year)	2.286	total	2.286	
nontraditional water resources’				
Shallow groundwater	.02			
Ruse of waste water	.077			
Total nontraditional water resources	.097			
Total available water	2.383			

Groundwater System

it is a part of the regional Nile Valley aquifer system. Eocene and Quaternary Aquifers are two main aquifers that forming a partially hydrological connected systems through several open vertical, inclined, and lateral channels, which are developed along faults, unconformities, and shifting slides [9].

Quaternary Aquifer

This is the primary aquifer in the field of study. It covers a large region, particularly on the Nile Valley's western side. This aquifer has a thick layer of sand and gravel mixed with clay lenses. Holocene Nile silt and sandy clays cover the aquifer, forming semi-permeable to impermeable strata. This top layer infiltrate water after irrigation in addition to subsurface seepage from irrigation canals and conduits. This layer's thickness ranges from zero (at the edges) to 16.5 meters (near the Nile reach), with an average thickness of 9 to 10 meters. [9].and porosity varies between 35% and 38% [10]. The

geometry of the Quaternary aquifer is characterized by steep inclination near the valley slopes with large extension in the North-South direction [11]. This aquifer is closed at the bottom by an impermeable clay bed of Pliocene age while at the Eastern and Western desert fringes it rests unconformably on Middle Eocene limestone [12, 13]. The thickness of the aquifer decreases from 200m South of Beni Suef to a few meters in the north (Fig 5). The aquifer is mostly renewed by Nile water infiltration from irrigation systems and cultivated land, but it may also be recharged by vertical upward leakage from earlier geologic aquifer systems with high-pressure heads (Aquifers of fissured Eocene limestone and Nubia sandstone complex) [14], and through the extended permeable layers and the fault planes. The aquifer losses its water either naturally through the seepage into the Nile River and irrigation drains, as well as, outflow into the other aquifer systems in contact, and evaporation from the surface, or abstraction of groundwater.

Eocene Aquifer

The Eocene rocks in the study area are mainly differentiated into Middle Eocene (mainly of limestone with shale or clay intercalations) that bound the Nile Valley from the east, and the Upper Eocene rocks (mainly of clays, marls with streaks of limestone) that bound the Nile Valley from the west. So, the Eocene rock units to the west of the Nile Valley have low groundwater potentialities compared to the East. [7, 14].

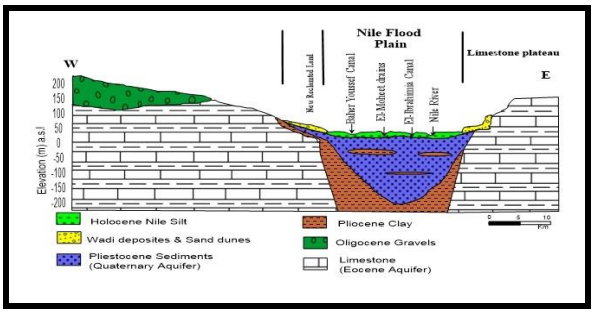

Figure 5. hydrogeological cross-section of Quaternary and Eocene aquifer at Beni Suef area after [15].

Methodology

Field and laboratory measurements were adapted to achieve this target. During February (2021), 26 groundwater samples were collected from drilled wells and 14 surface water samples. pH, Electric conductivity EC, salinity TDS, and Temp were all measured in situ using calibrated digital portable meters, Adwa AD11 and Adwa AD32. Groundwater and surface water samples were collected in one-liter acid-washed, well-rinsed, low-density polyethylene bottles, and chemical properties were determined using the American Public Health Association's standard. [16]. Filtration of the obtained samples was done using 0.45 µm micrometers membranes. For trace element analysis the Samples were acidified to a pH of less than 2 using ultrapure HNO_3. Major ions and trace elements were measured in groundwater and surface water samples. Titrations with standard EDTA were used to determine calcium (Ca^{+2}) and magnesium (Mg^{2+}). Chloride (Cl) was determined using a standard $AgNO_3$ titration, bicarbonate (HCO_3) was determined using an HCl titration, sodium (Na^+), and potassium (K^+) were determined using flame photometry, and phosphate, SO_4^{2-}, and NO_3^- were determined using a spectrophotometer. Evaporation and computation procedures were used to determine total dissolved solids [17]. An atomic absorption device was used to identify trace elements. All of the groundwater geochemical data used in this study was checked for charge balance using Geochemist's Workbench "commercial software" to ensure the quality of the studies. Groundwater analyses having a charge imbalance of more than 5% were excluded from the study. PHREEQC *[34]* was used to calculate ion activity, mineral speciation, and saturation indices. Table 2 shows the analytical results for the groundwater samples collected in the research region.

Results

Total dissolved salts (TDS)

The TDS values of groundwater varies from 591 mg/l to 6170 mg/l with an average 1331while the TDS values of surface water ranging from 204mg/l to 1670 mg/l whit an average 854.6 mg/l (Table 2). This increase in the total dissolved salts at surface water (El-Moheet drain and Baher Youssef sub-canal) is due to the indirect discharge of untreated sewage and agricultural drainage. The end of El-Ibrahimia canal is recharged from El-Moheet water with high TDS. Baher Youssef sub-canal that located at new reclaimed areas with high intensive use of fertilizers and dissolution of soil evaporites increase the TDS in the agricultural return water.

Major ions

The quantity of major ions (cations; such as Ca^{2+}, Mg^{2+}, Na^+ and K^+, and the anions; such as SO_4^{-2}, Cl^-, HCO_3^-, PO_4^{-3} and NO_3^-) in water is determined by the rock types or soil that contain the water. Additional sources of elements include industrial discharges, irrigation drainage, fertilizers, septic tanks, pesticides, and other anthropogenic-related sources. [18, 19]. According to the distribution of the highest concentration of major ions in the study area, they could be categorized into the following groups:
1) The first group comprises; K^+, Na^+, Ca^{+2}, , Mg^{+2}, Cl^-, SO_4^{2-}, · and NO_3^-,, where the maximum

concentrations are recorded in the central and Southern west of the study region. The concentration of K^+ ranges between 4 and 38 mg/l with a mean value of 9.93 mg/l. Na^+ varies from 115 to 1600 mg/l averaging 296.4 mg/l (Table 2). Mg^{2+} from 18 to 101.8 mg/l averaging 39.44 mg/l while Ca^{2+}varies from 51 to 433 mg/l with an average of 135.9 mg/l (Table2) The concentration of Cl^- ranges from 27.4 to 2287 mg/l with an average of 285.2 mg/l (Table 2). SO_4^{2-} varies from 31 to 985 mg/l with an average of 221.8 mg/land the concentration of NO_3^- ranges from< 0.2 to 158.8 mg/l with a mean value 12.59 mg/l (Table 2).

2) The second group involvesPO_4^{3-} and HCO_3^- .concentrations of PO_4^{3-} and HCO_3^-ions are high at the Eastern part of the study area. HCO_3^- varies from 295 to851 mg/l with a mean value of 522.6 mg/l (Table 2).

The low salinity and major element concentrations in the Eastern side of the study area can be attributed to the positive hydrochemical impact of the El-Ibrahimia canal and its branches in diluting groundwater salinity, whereas the western drainage systems of Baher Youssef, and El-Moheet have the opposite effect on groundwater

Table 2. summary of chemical analysis of groundwater and surface water associated with standards [24]

	Groundwater				Surface water			Average
Parameters	Unit	Min	Max	Average	Min	Max	average	acceptable [24]
pH field	_	7.2	8.2	7.68	7.6	8.6	8.18	_
K	mg/l	4	38	9.93	5	10	7	_
Na	mg/l	115	1600	269.4	28	386	162.6	200
Ca	mg/l	51.7	433.8	135.9	27.2	153.2	79	200
Mg	mg/l	18	101.8	39.44	10.2	48.6	27.34	150
Cl	mg/l	27.4	2287	285.2	11.15	581	184.1	250
HCO3	mg/l	295	851	522.6	141	612	280.3	_
TDS	mg/l	591	6170	1331	204	1670	854.6	1000
EC	µS/cm	338	9670	2017	319	2610	1336	2500
Ba	mg/l	0.013	0.202	0.0903	0.012	0.13	0.0672	0.7
F	mg/l	0.08	0.76	0.3096	0.32	0.75	0.526	_
SO4	mg/l	31	985	221.8	24.8	284	150.3	250
NO3	mg/l	<0.2	158.8	12.59	0.44	40.2	14.73	10
Cr	ug/l	<2	11	4.41	<2	11	8.07	50
Pb	ug/l	<7.0	<7.0	<7.0	<7.0	<7.0	<7.0	10
Meas_Alk	mg/L	295	851	522.6	141	612	280.3	_
NO2	mg/l	0	8.65	0.48	0	13.83	1.717	_
Fe	mg/L	<0.006	1.59	0.322	0.034	0.97	0.296	0.2
Cu	ug/L	<6	156	33.5	<6	235	65.8	2000
Mn	mg/L	0.042	1.71	0.603	0.031	1.2	0.337	0.05
Ni	ug/L	<4	7	2.48	<4	11	4.86	20
Se	ug/L	<7.0	<7.0	<7.0	<7.0	<7.0	<7.0	10
V	ug/L	<1.0	20	5.61	<1.0	30	15.25	100
Sb	ug/L	<9.0	<9.0	<9.0	<9.0	<9.0	<9.0	20
Al	ug/l	<7	396	52.6	<7.0	764	190.8	200
Cd	ug/l	<2	11	4.444	<2	15	7.86	1
Zn	ug/l	<5.0	114	29.46	<5.0	132	47.9	15
As	ug/l	<6	<6	<6	<6	<6	<6	4

Hydrogeochemical facies

It is obvious from the piper diagram [20] that about of 16 samples, 40 % of the samples fit in Ca^{+2}– Mg^{2+}– HCO_3^- type, and 35 % samples fall at Na^+- Cl^-- SO_4^{-2} Saline type, showing the change of the Nile water from Mg^{+2}– Ca^{+2}– HCO_3^- type temporary hardness to Na^+– Cl^-–SO_4^{-2}Saline type by the dissolution of evaporites and evaporation process. The dissolution of evaporites leads to a progressive increase of SO_4^{2-} and Cl^- compared with HCO_3^- . with an of Na^+ increase relative to $Ca^{+2}$and Mg^{2+} from 1 to3 (Fig. 6). Also seen in (Fig. 6) the most of groundwater samples (25%) are in zone 5, the mixed zone, where neither anion nor cation dominating groundwater types can be recognized. Ternary diagram of cations (Na+K – Mg – Ca) as well as anions (Cl–SO_4 – HCO_3) at piper diagram illustrating that the geochemical evolution of the source water (Nile water) along its path from the surface to groundwater from Ca^{+2}apex to Na^+ apex and from HCO_3^- apex to both of $SO_4^{-2}$and Cl, therefore, it's a good evidence of evaporites (halite and gypsum) dissolution.

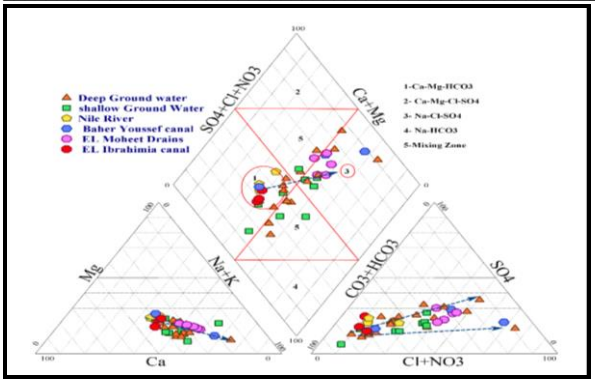

Figure 6 . Piper plot of the different water type.

Hydrogeochemical classification

Geochemistry of water is affected by rock types, environment, and water flow. [21, 22]. As a result, Chadha proposes a hydrogeochemical diagram to differentiate the types of water-rock interaction processes in aquifers. [23] study and classified water type and its controlling processes by applying these relation the difference in milliequivalent percent between (Ca^{+2} + Mg^{+2}) and (K^{+} + Na^{+}) on the horizontal axis, and the difference between (CO_3^{-2} + HCO_3^{-}) and (SO_4^{-2} + Cl^{-}) on the vertical axis. The geochemical compositions of the surface and ground waters represent four discrete water types (Fig. 7). These are generally as reverse cation-exchange (Ca–Mg–Cl), Recharging from Nile water (Ca–Mg–HCO_3^{-}), evaporites dissolution (Na-Cl-SO_4), and normal cation exchange water (Na–HCO_3 type). Geochemical analyses of the river water samples have been added to the processed groundwater data to show how recharge must have evolved geochemically as it became groundwater and to help explain the relation between the surface water and groundwater.

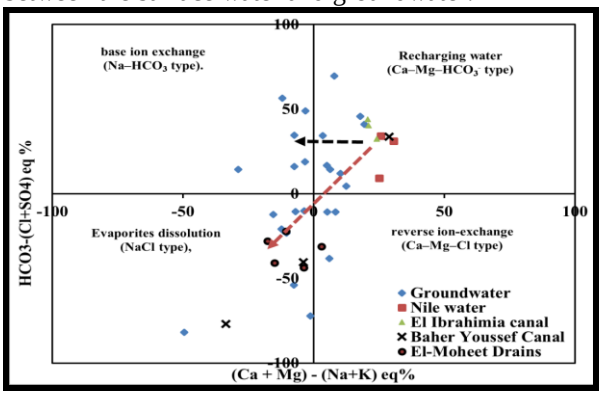

Figure 7 . Piper plot of the different water type.

Trace elements

According to the limits imposed by [24], trace elements quantities (copper , chromium , and other metals) in groundwater are safe for domestic and drinking usage except manganese, iron, and cadmium, are all above the safe levels. The concentration of iron ranges between <0.006 and 1.59 mg/L with a mean value 0.322 mg/L which is relatively high for drinking. Most of the groundwater in the region is characterized by high iron (> 0.2 mg/L). while low (< 0.2 mg/L) at the North side. Aluminum concentration fluctuates from <0.7 µg/L to 396 µg/L (Table 2) with a mean value 52.6 µg/L. Aluminum concentration at surface water ranging from < 7.0 µg/L to764 µg/L with an average of 190.8 µg/L. The manganese content ranges between0.042 mg/L to 1.71 mg/L with an average of 0.603 mg/L (Table2).

Discussion

Geochemistry of surface water controlling mechanism

The Gibbs diagram [25] can be applied to estimate the controlling mechanism of surface water chemistry, which proposes that three mechanisms (evaporation-crystallization process, rock weathering, and the atmospheric precipitation.) are the main processes controlling the composition of dissolved salts in the waters. The results of the studies (Table 2) are plotted on the Gibbs diagram (Fig. 8) to show that rock weathering and surface water and soil water evaporation is the main mechanism in the evolution of surface water chemical composition, leading to greater salinity.

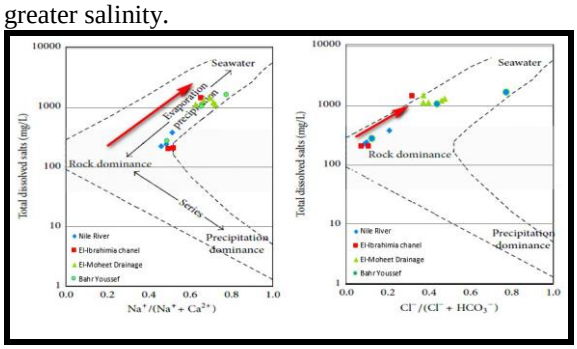

Figure 8. Gibbs plot illustrating main processes controlling surface water chemistry.

Hydrogeochemical processes

Water rock interaction

Dissolution of Carbonate and Gypsum

chemistry of groundwater investigation revealed that the major ions in groundwater include Na^{+}, Ca^{+2}, Cl, Mg^{2+}, HCO_3 and SO_4^{-2}. These main ions are usually found in groundwater due to the dissolution of carbonates and evaporites in aquifers. The following is a summary of several geochemical processes that might be occurring in the aquifer:

The dissolution of dolomite would release equivalent charge of (Ca^{+2} + Mg^{2+}) and HCO_3^{-} Equations (2) and its ratio should be 1:1 (Fig. 9.b). also the dissolution of calcite would release equivalent charge of Ca^{+2} and HCO_3^{-} Equations (1) and its ratio should be 1:1 (Fig. 9.a). concurrent dissolution of dolomite and

calcite would give equivalent ratio of Ca^{+2} and HCO_3^- between 1:1 to 1:2 line (Fig. 9.a). Furthermore, at (Fig.9.a) some samples located above the 1:1 line so it revealed that the extra Ca^{+2} may be come from another source, such as gypsum mineral dissolution or ion exchange among Ca^{+2} and Na^+. Extra Ca^{+2} would be released into groundwater when gypsum dissolves (Equation.6).

The equivalent ratio between $Ca^{+2}$and SO_4^{-2} was more than 1, revealed that gypsum dissolution was one of the sources of extra Ca^{+2} in groundwater (Fig. 9 d). The equivalent ratios of (Ca^{+2} + Mg^{2+}) with (SO_4^{-2}+ HCO_3^-) estimate that the contribution of carbonate and gypsum mineral dissolution to groundwater chemistry (Fig. 9.c) if the samples were arranged along a 1:1 line, carbonate and gypsum dissolution would be the only source of Ca^{+2}, Mg^{2+}, $SO_4^{-2,}$ and HCO_3. the majority of samples fall below the 1:1 line of (Ca^{+2}+ Mg^{2+}) and (HCO_3 + SO_4^{2}), indicating carbonate precipitation (consuming Ca^{+2}, Mg^{2+}, HCO_3) and gypsum dissolution (increasing SO_4^{2}).

Table 3. Different geochemical reactions that could be operating in the aquifer.

Process	Geochemical reaction	Reaction
Congruent dissolution of calcite	$CaCO_3 + H_2CO_3 \rightarrow Ca^{2+} + 2HCO_3^-$ $CaCO_3 + H^+ \rightarrow Ca^{2+} + HCO_3^-$	1 1a
Congruent Dissolution of dolomite	$CaMg(CO3)_2 + 2H_2CO_3 \rightarrow Ca^{2+} + Mg^{2+} + 4HCO_3^-$ $CaMg(CO_3)_2 + 2H^+ \rightarrow Ca^{2+} + Mg^{2+} + 2HCO_3^-$	2 2a
Incongruent dissolution of dolomite	$CaMg(CO_3)_2 + {}_2H_2CO_3 \rightarrow CaCO_3 + Mg^{2+} + 2HCO_3^-$ $CaMg(CO3)2 + H^+ \rightarrow CaCO3 + Mg^{2+} + HCO_3^-$	3 3a
Biological processes and atmospheric gas	$CO_2 + H_2O \rightarrow H_2CO_3 \leftrightarrow H^+ + HCO_3^-$	4
Sulphate Reduction	$CH_2O + 1/2\ SO_4^{-2} \rightarrow 1\ H_2S^- + HCO_3^- + 1\ H_2^+$	5
Dissolution of gypsum	$CaSO_4.2H_2O \rightarrow Ca_{(aq)}^{2+} + SO^2{}_{4(aq)}^- + 2H_2O$	6
Normal cation exchange process.	$Ca^{2+}(aq) + 2Na\text{-}X \rightarrow 2Na^+(aq) + Ca\text{-}X_2$	7
Na^+ exchange by Ca^{2+}	$(Ca) - Ex + 2Na^+(aq) \rightarrow Ca^{2+}(aq) + (2Na) - Ex$	8
Na^+ exchange by Mg^{2+}	$(Mg) - Ex + 2Na^+(aq) \rightarrow Mg^{2+}(aq) + (2Na) - Ex$	9
Mg^{2+} exchange by Ca^{2+}	$Mg - Ex + Ca^{2+}(aq) \rightarrow Mg^{2+}(aq) + Ca^{2+} - Ex$	10
Iron sulphide oxidation	$15/4\ O + FeS_2\ (s) + 7/2\ H_2O \rightarrow Fe(OH)_3(s) + 2SO^2{}_4^- + 4H^+$	11
Nitrification	$O_2 + 1/2NH_4^+ \rightarrow 1/2\ {}_3NO^- + H^+ + 1/2\ H_2O$	12
Carbonate precipitation	$Ca^{+2} + 2HCO_3^- \rightarrow CaCO_3\ (S) + H_2CO_3$	13
Halite dissolution	$Na\ Cl \rightarrow Na^+ + Cl^-$	14

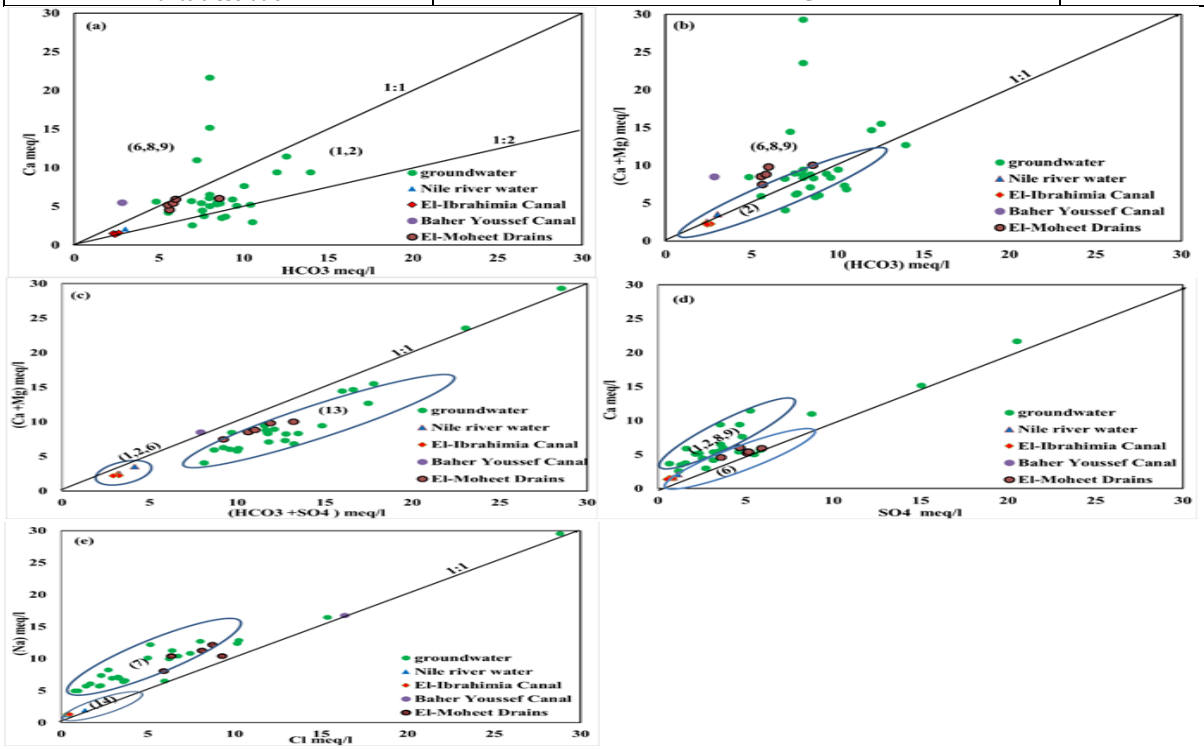

Figure 9. binary graphs showing Relationships between major ionsand the controlling processes on the geochemistry of groundwater samples. **(a)** relation between Ca^{2+} with HCO_3^-,and showing calcite dissolution. **(b)** (Mg^{2+} + Ca^{2+}) with (HCO_3^-) showing dolmite dissolution **(c)** (Ca^{2+}+Mg^{2+}) with (HCO_3^-+SO_4^{2-}),**(d)** (Ca^{2+}) with (SO_4^{-2}),**(e)** Na^+ and Cl^-

.The relation between non-carbonate mineral-derived Ca^{+2} and Mg^{+2} and SO_4^{-2} also investigated by [26] using the equation $[(Mg^{+2} + Ca^{+2}) - 0.5(HCO_3\text{-})]$ plotted against SO_4^{-2} to see how sulphate mineral dissolution affects the concentration of Ca^{+2} in groundwater. Sulfate mineral dissolution appears to have impacted nearly all surface and groundwater (correlation coefficients, R^2, of groundwater, Nile water, El Ibrahimia canal, Bahr Youssef, and El Moheet drains are (0.93,.95,.69,.97, and.95, respectively) (Fig. 10). The strong positive correlation between (Ca+Mg)-.5HCO3) and SO4, as well as the increase in Ca+2 with SO4-2, suggests that gypsum weathering is a source of Ca^{+2} and SO_4^{-2}.

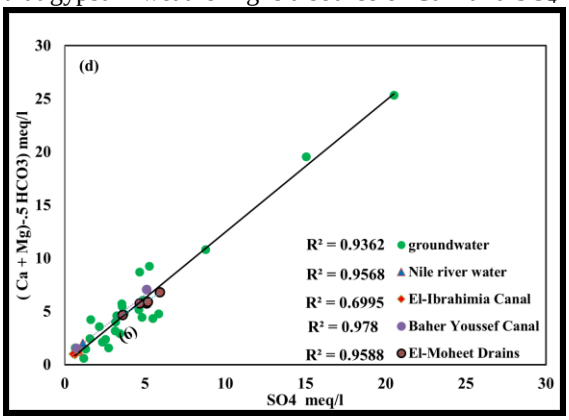

Figure 10. Geochemical cross-plots of all water systems. concentration of noncarbonate magnesium and calcium with. sulphate; non-carbonate calcium is $(Ca^{2+} + Mg^{2+}) - 0.5(HCO_3^-)$.

Halite Minerals Dissolution

PCA results revealed that PC1 had a high loading to Cl^- and Na^+. One of the main sources of (Na+ and Cl) in groundwater was halite dissolution (equation4, Table .3). If the aquifer's main source of (Na^+ and Cl^-) was the dissolution of halite, the ratio of (Na+ / Cl) should be near to 1:1. According to (Fig. 9e) it was assumed that halite dissolution was a major source of (Na+ and Cl) in groundwater. most of the groundwater samples, however, were found to be above the 1:1 line of (Na+ / Cl). This explains that extra Na+ in groundwater might come from a variety of processes, including ion exchange and anthropological activities, in addition to halite dissolution. Furthermore, all groundwater samples had saturation indices values of halite that were fewer than 0, indicating that the water samples were undersaturated in halite. As a result, halite dissolution might occur in the investigation area.

Cation Exchange

it is a significant process that influences the evolution of groundwater's hydrochemical properties [27]. to estimate the role of cation exchange proceeding in the aquifer The ratio of $\{[(Ca^{2+} + Mg^{2+}) - (SO_4^{2-} + HCO_3^-)] / (Na^+ - Cl^-)\}$ is usually used [28, 29]. (Fig. 11a) shows that for most groundwater samples, the value of $\{[(Ca^{2+} + Mg^{2+}) - (SO_4^{-2} + HCO_3^-)] / (Na+ Cl)\}$ were near to 1, indicating that cation exchange is an important factor controlling the groundwater geochemical composition. [30]. The cation exchange computed by the Chloro-Alkaline indices (CAI) [27]. The value of $[Cl - (Na^+ + K^+)]/Cl$ is known as CAI-I. CAI-I with a positive value shows reverse ion exchange between Na^+ in water replace (Ca^{2+} and Mg^{2+}) in the aquifer Formation, whereas CAI with a negative value suggests normal ion exchange between (Ca^{2+} and Mg^{2+}) in water replace (Na^+ and K^+) in the aquifer medium. CAI-I values for all water samples were less 0. in this case, Ca^{+2} enter aquifer medium and release Na+ water from (Fig. 11b).

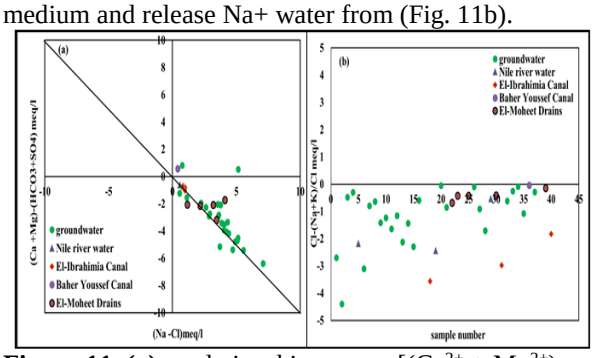

Figure 11. (a) a relationship among $[(Ca^{2+} + Mg^{2+}) - (SO_4^{2-} + HCO_3^-)]$ and $(Na^+ - Cl^-)$ that confirm the presence of the cation exchange process of the water samples **(b)** Chloro-Alkaline indices (CAI) which indicate that normal cation exchange process (Ca^{+2} release Na^+ from aquifer medium).

Anthropogenic activities

the usage of chemical fertilizers, waste disposal, and wastewater discharges have been shown to affect the chemical composition of water in previous research [5, 31, 32]. The results of PCA in this study also demonstrated that human activities may have an impact on groundwater hydrochemistry. The quantity of NO_3 in several groundwater samples was found to be high, and they mostly occurred around agricultural and urban areas, most likely due to sewage and exhaustive agriculture activities. The correlations among NO_3^- and physiochemical measures might be used to determine how human activities affect groundwater quality. The correlation study revealed that NO_3 and Cl had a strong relationship (the correlation coefficient was 0.895, Table .4). Furthermore, both (Cl and NO_3) have a significant PC1 loading. consequences revealed that (Cl and NO_3) came from comparable sources, confirming the contaminant's anthropogenic source.

Mineral Dissolution and its Saturation Index

Groundwater geochemistry was influenced by a

number of factors, including groundwater fluxes, recharge, and discharge processes, as well as water-rock interactions. Mineral weathering has an effect on hydrochemistry along the groundwater flow direction when it has been in place for a long period [33]. The mineral saturation index can be computed using the equation SI = log (K_{IAP} /K_{SP}) (where, K_{IAP} is the ions activity product for a mineral equilibrium reaction, and K_{SP} is the solubility product of the mineral). the SI values of minerals in groundwater could be computed by using The PHREEQC program [34]. If the (SI < 0) the water is unsaturated to the mineral and dissolve it continually; if (SI > 0) the water is supersaturated to the mineral and it will precipitate it; and if SI of water is near to 0, the water will remain in equilibrium with mineral phase. The saturation indices of specific minerals were computed using hydrochemistry data (Table 5). Except for two surface water samples (5,18), the Saturation Index values of dolomite and calcite were larger than 0, meaning that carbonate minerals had progressed from under saturation to supersaturation. While the SI of gypsum and halite in all water samples was fewer than zero (Table5), this indicates that the halite and gypsum will continue to dissolve in the groundwater Calcite and dolomite Saturation Index values varied from 0.27 to 1.24 and 0.67 to 2.37, respectively, with mean values of 0.57475 and 1.00350. (Fig. 12a) demonstrates that SI of calcite and dolomite has a weak positive correlation with TDS, whereas SI of (Halite and Gypsum) has a high positive correlation with TDS. Furthermore, (Ca^{+2}, HCO_3) and (Ca^{+2}, Mg^{+2}, HCO_3) concentrations do not correlate with SI calcite and SI dolomite (Fig. 12b, c), showing that part of the minerals will not continue to dissolve along flow path of the groundwater. SI halite and SI gypsum, on the other hand, were less than 0 and correlated with TDS positively (Fig. 12a). Also, strong correlation coefficients exist between Na^+ and Cl^-, Ca^{2+}, and SO_4^{-2} (R^2 = 0.989 and 0.925, respectively, (Table 4). This indicates that the dissolution of halite and gypsum will continue. At the same time, the accumulation of Ca^{+2} from gypsum dissolution might cause supersaturation of calcite and dolomite, limiting calcite and dolomite. The scatter plots of Na^+, Cl^-, and SI halite are shown in (Fig.12 e). Ca^{+2}, SO_4^{+2}, and SI gypsum are shown in (Fig.12d), with R^2 values of 0.96, 0.98, 0.904, and 0.97, respectively.

.

Table 4. correlation matrix showing the relation between major ions with each other.

	K^+	Na^+	Ca	Mg	Cl	SO4	HCO_3	NO3	Fe	(TDS)
K^+	1	0.136	.342	.269	.180	.381	-.012	.041	.055	.199
Na	.136	1	.742	.849	.989	.798	.268	.896	-.016	.990
Ca	.342	.742	1	.861	.748	.925	.484	.507	.098	.818
Mg	.269	.849	.861	1	.834	.877	.458	.694	.138	.895
Cl	.180	.989	.748	.834	1	.821	.160	.895	-.007	.983
SO4	.381	.798	.925	.877	.821	1	.227	.603	.127	.858
HCO3	-.012	.268	.484	.458	.160	.227	1	.066	.134	.320
NO3	.041	.896	.507	.694	.895	.603	.066	1	.007	.861
Fe	.055	-.016	.098	.138	-.007	.127	.134	.007	1	.037
(TDS)	0.199	0.990	.818	.895	.983	.858	.320	.861	.037	1

Table 5. summary of Saturation incises of mineral phases (carbonate, gypsum, and halite).

Saturation Index of Mineral phases	Minimum	Maximum	Mean	Std. Deviation
Anhydrite	-2.730	-.620	-1.74175	.481131
Aragonite	-.420	1.100	.43075	.345360
Calcite	-.270	1.240	.57475	.344874
Dolomite	-.670	2.370	1.00350	.668487
Gypsum	-2.510	-.400	-1.52250	.480260
Halite	-8.040	-4.160	-6.32425	.876578

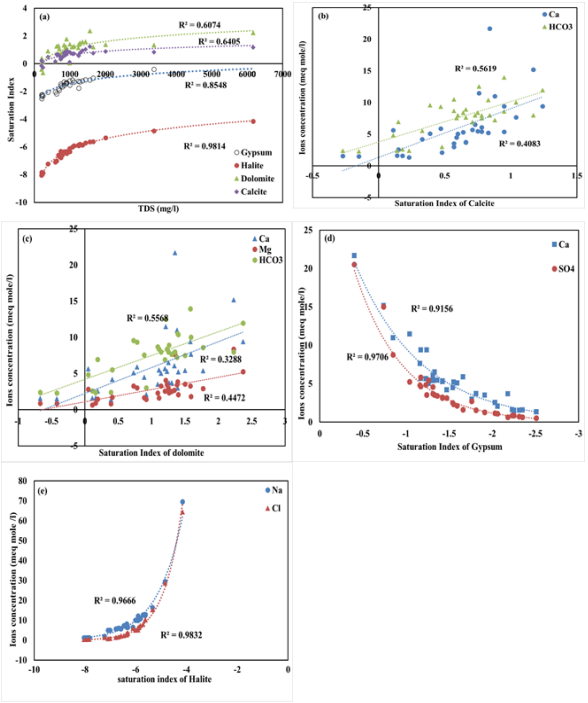

Figure 12 . (SI) plots of selected mineral phases with TDS or ion concentration. **(a)** SI for (halite, gypsum, calcite, and dolomite) against TDS, **(b)** (Ca^{+2}, HCO_3^-) with. SI calcite, **(c)** (Ca^{+2}, Mg^{2+}, HCO_3^-) vs. SI dolomite, **(d)** Ca^{+2}, SO_4^{2-} vs. SI gypsum, **(e)** Na^+, Cl^- vs. SI halite.

Principal Component Analysis of Hydrochemistry

Table 6 shows the relationships between the nine factors. Most variables have a strong correlation with more than one other variable. According to the PCA results, two PCs (PC1 and PC2) with eigenvalues larger than 1 could explain 82.8 percent of the total data variability (Table6). PC1 and PC2 were accounted for 68.49% and 14.33% of the overall variation, respectively. PC1 has significant positive loadings of (Na^+, Mg^{+2}, Ca^{+2}, SO_4^{-2}, NO_3^- Cl^-, and TDS), with loadings of 0.974, 0.696, 0.791,.982,.805,.93 and 0.96, respectively. At PC1 three high loading relationships is showing different scenarios. The first (Ca^{+2}, Mg^{+2}, SO_4^2, and TDS) represented the dissolution/precipitation of carbonate and sulphate minerals, whereas the second (Cl and NO_3). Nitrate is a widespread groundwater contaminant that originates mostly from urban sewage and agricultural [35, 36]. Consequently, PC1 indicated the impact of human activities. The third (Na^+ and Cl) is mostly owing to the halite dissolution, which results in an enrichment of Na^+ and Cl. PC2 was mostly related to high levels of K+, Mg^2, Ca^{+2} $^+$, and HCO_3, indicating interactions between infiltrating water and dolomite. The mineral dissolution (such as halite, carbonates, and gypsum minerals) as well as human activities altered the hydrogeochemical characteristics of groundwater.

Table (4) shows the results of the major hydrochemical parameter correlation. The high positive relationships among TDS and a variety of ions (Mg^{2+}, Cl, Na^+, SO_4^2, Ca^{+2}, and NO_3) show that these ions play an essential role in the geochemical evolution of groundwater. There are strong relationships between (Cl and Na^+) =(0.989), (SO_4^2 and Ca^{+2}) =(0.925), and (Mg^{2+} and Ca^{+2}) =(0.861), indicating that gypsum, halite, and carbonate dissolution may be the source of the main ions in groundwater.

Table 6. Loadings for Varimax rotated factor matrix of the chemical datasheet (significant loadings are marked by*****).

Rotated Component Matrix		
	Component	
	1*	2*
Potassium K	.045	.687
Sodium Na	.974*	.146
Calcium Ca	.696*	.634*
Magnesium Mg	.791*	.535*
Chloride Cl	.982*	.121
Sulfate SO4	.805*	.425
Bicarbonate HCO3	.095	.729*
Nitrate NO3	.930*	-.116
Total Dissolved Solids (TDS)	.960*	.257
Eigenvalue	6.16	1.29
Explained Variances %	68.49	14.33
Cumulative % of variances	68.49	82.833
Extraction Method: Principal Component Analysis. Rotation Method: Varimax with Kaiser Normalization.		
a. Rotation converged in 3 iterations.		

Conclusion

Many samples were taken from the flood plain aquifer and surface water that include the Nile River, Bahr Youssef canal, El-Ibrahimia canal, as well as drainage and irrigation canals, to study the geochemical evolution of Nile water on its way to reach and recharge its flood plain aquifer. The water type evolved along its way from fresh Ca–Mg–HCO3 water at the recharging source of water (mainly Nile river and its branches El-Ibrahimia canal and Bahr Youssef), to high salinity Na–Cl–SO4 drainage waters of El Moheet drains, as well as some groundwater on the western side of the study region. The evaporites dissolution such as halite and gypsum from the Eastern side of the study area (newly reclaimed land) and the impact of unsupervised human activities such as intensive use of pesticides, fertilizers, industrial waste, waste disposal, leakage from septic tanks, and evaporation control these evolutions. Excluding Nile water, the results of the water saturation index in the research region revealed that groundwater was saturated to supersaturated for calcite and dolomite. This is because the Nile water dissolve carbonate mineral along its way to reach the groundwater, whereas undersaturated for the main evaporites (halite and gypsum) mineral phases. Therefore, deposition of carbonate minerals and dissolution of the evaporites are expected. The results of the PCA, Chadha diagram, and piper plotting, combined with the saturation index, suggested that rock weathering, as the dissolution of halite and gypsum minerals, precipitation of calcite and dolomite, ion exchange between [(Mg^{2+} Ca^{2+}) and Na^{+}], and human activities such as sewage and excessive practices of agriculture, influenced the hydrogeochemical evolution of groundwater in the study area.

References

1. EL Sayed, M.A.A., Delineating the Quaternary aquifer in apart of the Nile Valley using D. C. Electrical Soundings: Egypt. Jour. Geol., Vol. 24 No. 1-2 pp. 53-100 . 1991.
2. Lawrence, A., et al., Groundwater evolution beneath Hat Yai, a rapidly developing city in Thailand. 2000. **8**(5): p. 564-575.
3. Edmunds, W., et al., Groundwater recharge history and hydrogeochemical evolution in the Minqin Basin, North West China. 2006. **21**(12): p. 2148-2170.
4. Awad, S., Environmental studies on groundwater pollution in some localities in Egypt. 1999, Ph. D. thesis, Faculty of science, Cairo University, Egypt.
5. Melegy, A., et al., Hydrogeochemical characteristics and assessment of water resources in Beni Suef Governorate, Egypt. 2014. **2014**.
6. Said, R., The geological Evolution of River Nile, Spring-Verlag, New York. 1981, Inc.
7. Tamer, M.A., Geology of El Fayum, Beni Suef Regions: Bull. Desert Inst. Egypt, Vol. 25, N. 1, 2, pp. 27- 47. . 1974.
8. Tamer, A., M. El Shazly, and A.J.T.D.I.B. Shata, ARE, Geology of El-Faiyum-Beni Suef region [Egypt]. 2. Stratigraphy. 1975.
9. Abou Heleika, M., S. Toney, and E.J.A.J.o.G. Ismail, Mapping of groundwater opportunities for multi-purposes use in Beni-Suef province, Egypt. 2021. **14**(9): p. 1-18.
10. Korany, E.A. and S.A. Hussein, Geohydrologic status and control of land and water management in the reclaimed desert area, west of Nile Valley, Egypt. Proc. -142 1982.
11. Sayed, M.A.A., Geophysical study on the area between Cairo and Beni Mazar in relation to groundwater and oil possibilities: Ph. D.Thesis. Fac. Sc., Ain Shams Univ., Cairo 198 P. . 1977.
12. (RIGW/IWACO), R.I.f.G., Legends and layouts for hydrogeological mapping, 1:100.000. Technical Note 70. 55p. Project "Development and Management of groundwater Resources in the Nile Valley and Delta". 1989.
13. (RIGW), R.I.f.G., Hydrogeological map of Egypt, Scale 1: 500,000, Sheet of Beni Suef, Explanatory Note 13p. 1997.
14. Korany, E., A. Statistical approach in the assessment of the geohydrologic profiles. in 9th International Congress. Statistics, Computer. Sciences. Social and Demerges Research, Cairo, Ain Shams University Press, Egypt. 1984.
15. (RIGW/IWACO), R.I.f.G., Hydrogeological map of Egypt, scale 1:100000, 2nd ed., Map Sheet of El-Minia, Research Institute for Groundwater. 1992.
16. Walter, W.G., Standard methods for the examination of water and wastewater. 1961, American Public Health Association.
17. Hem, J.D., Study and interpretation of the chemical characteristics of natural water. Vol. 2254. 1985: Department of the Interior, US Geological Survey.
18. El Kashouty, M.J.A.J.o.G., Modeling of limestone aquifer in the western part of the River Nile between Beni Suef and El Minia. 2013. **6**(1): p. 55-76.
19. Melegy, A.A., et al., Geochemical mobilization of some heavy metals in water resources and their impact on human health in Sohag Governorate, Egypt. 2014. **7**(11): p. 4541-4552.
20. Piper, A.M.J.E., Transactions American Geophysical Union, A graphic procedure in the geochemical interpretation of water-analyses. 1944. **25**(6): p. 914-928.
21. Ravikumar, P. and R.J.A.W.S. Somashekar, Principal component analysis and hydrochemical facies characterization to evaluate groundwater

quality in Varahi river basin, Karnataka state, India. 2017. **7**(2): p. 745-755.
22. Raju, N.J.J.E.G., Hydrogeochemical parameters for assessment of groundwater quality in the upper Gunjanaeru River basin, Cuddapah District, Andhra Pradesh, South India. 2007. **52**(6): p. 1067-1074.
23. Chadha, D.J.H.j., A proposed new diagram for geochemical classification of natural waters and interpretation of chemical data. 1999. **7**(5): p. 431-439.
24. (WHO), W.H.O., Guidelines for drinking-water quality: fourth edition incorporating the first addendum. Geneva:
World Health Organization, Licence: CC BY-NC-SA 3.0 IGO. 2017.
25. Gibbs, R.J.J.S., Mechanisms controlling world water chemistry. 1970. **170**(3962): p. 1088-1090.
26. Kimblin, R.J.J.o.H., The chemistry and origin of groundwater in Triassic sandstone and Quaternary deposits, northwest England and some UK comparisons. 1995. **172**(1-4): p. 293-311.
27. Charfi, S., et al., Study of variation in groundwater quality in a coastal aquifer in north-eastern Tunisia using multivariate factor analysis. 2013. **302**: p. 199-209.
28. Huang, G., et al., Impact of anthropogenic and natural processes on the evolution of groundwater chemistry in a rapidly urbanized coastal area, South China. 2013. **463**: p. 209-221.
29. Wang, H., et al., Hydrogeochemical characterization of groundwater flow systems in the discharge area of a river basin. 2015. **527**: p. 433-441.
30. Li, P., J. Wu, and H.J.A.J.o.G. Qian, Hydrochemical appraisal of groundwater quality for drinking and irrigation purposes and the major influencing factors: a case study in and around Hua County, China. 2016. **9**(1): p. 1-17.
31. Zghibi, A., et al., Understanding groundwater chemistry using multivariate statistics techniques to the study of contamination in the Korba unconfined aquifer system of Cap-Bon (North-east of Tunisia). 2014. **89**: p. 1-15.
32. Omo-Irabor, O.O., et al., Surface and groundwater water quality assessment using multivariate analytical methods: a case study of the Western Niger Delta, Nigeria. 2008. **33**(8-13): p. 666-673.
33. Wen, X., Y. Wu, and J.J.E.g. Wu, Hydrochemical characteristics of groundwater in the Zhangye Basin, Northwestern China. 2008. **55**(8): p. 1713-1724.
34. Parkhurst, D.L. and C.J.W.-r.i.r. Appelo, User's guide to PHREEQC (Version 2): A computer program for speciation, batch-reaction, one-dimensional transport, and inverse geochemical calculations. 1999. **99**(4259): p. 312.
35. Yang, P., et al., Formations of groundwater hydrogeochemistry in a karst system during storm events as revealed by PCA. 2010. **55**(14): p. 1412-1422.
36. Yang, P., et al., Sources and migration path of chemical compositions in a karst groundwater system during rainfall events. 2013. **58**(20): p. 2488-2496.